Jurnal Teknik Informatika Vol. 19 No. 1, April 2026 (1-11)
ISSN: p-ISSN 1979-9160 (Print)| e-ISSN 2549-7901 (Online)
DOI: https://doi.org/10.15408/jti.v19i1.47091

JURNAL TEKNIK INFORMATIKA
Homepage : http://journal.uinjkt.ac.id/index.php/ti

Automatic Detection of Foot Arch Using Clarke's Angle Calculation Through a Web-Integrated System for Children

Shobiha Awwaliyah[1], Qalbi Rivantona[2], Alfaturachman Maulana Pahlevi[3], Dedi Nurcipto[4*], Menik Dwi Kurniatie[5]

[1,2,4,5]Biomedical Engineering, Faculty of Engineering, Dian Nuswantoro University
[3]Informatics Engineering, Faculty of Informatics, Dian Nuswantoro University
[1,2,3,4,5] Building I, Nakula 1 Street No.5-11, Pendrikan Kidul,
Semarang Tengah, Semarang City, Central Java 50131

Article:
Accepted: March 13, 2026
Revised: January 11, 2026
Issued: April 30, 2026

***Correspondence Address:**
dedi.nurcipto@dsn.dinus.ac.id

ABSTRACT

Foot deformities, particularly flatfeet (pes planus), are frequently observed in children. Although many children exhibit some form of flatfeet, this condition can persist and cause biomechanical issues, pain, and postural misalignments. Early detection and monitoring of foot arch development are critical to preventing long-term complications. However, common diagnostic methods such as wet foot print tests, X-rays, and MRIs are costly, time-consuming, and involve radiation exposure. This study proposes an innovative web-based system that detects foot arch types in children using Clarke's Angle. The system employs digital image processing to calculate the arch angle, offering a non-invasive, efficient, and cost-effective alternative to existing methods. The system was tested on 180 children aged 2-7 years at two locations in Semarang: Kindergarten & Daycare Habibie Ainun Tlogosari and Integrated Service Post Kemuning. The results from the Clarke's Angle measurements from the web-based system were compared with the wet foot print test, showing minimal differences and achieving an accuracy rate of 98.89%. This system offers a reliable solution for early detection and is suitable for use in both clinical and community health settings. It provides a faster, more accessible approach to pediatric foot assessment, delivering real-time results and eliminating any waiting time.

Keywords : *Clarke's Angle; flatfeet; pediatric foot diagnosis; image processing; foot arch classification.*

Jurnal Teknik Informatika Vol. 19 No. 1, April 2026 (1-11)
ISSN: p-ISSN 1979-9160 (Print)| e-ISSN 2549-7901 (Online)
DOI: https://doi.org/10.15408/jti.v19i1.47091

1. INTRODUCTION

Flat feet or pes planus is an anatomical condition characterized by a reduction or loss of the medial longitudinal arch (MLA) when the foot supports body weight. In children, this condition is often part of a physiological developmental stage that can improve over time [1]. However, in many cases, flat feet can be persistent and develop into a pathological condition that triggers complex disorders. This condition is not merely about having flat feet, but can be the starting point for whole-body biomechanical disorders, causing ongoing discomfort, postural changes, and potentially impacting adulthood if not properly addressed[2][3]. Flat feet that are not treated properly can affect a child's gait or walking pattern, increase the risk of joint pain, especially in the knees, and cause poor posture that can impact further development [4][5].

In flat feet, changes in the structure of the foot bones often involve a decrease in the height of the arch, which causes increased pressure on the medial part of the foot, disrupting weight distribution during walking [6]. This can potentially increase the risk of other musculoskeletal problems, including knee pain, ankle pain, and spinal problems. Flat feet can cause valgus deformity of the spine, which increases the load on the knee and ankle joints, worsening structural abnormalities in the long term [1][7]. Conversely, feet with pes cavus (high arches) experience uneven weight distribution, causing pain in the soles of the feet and posture problems due to excessive tension on the tendons and ligaments [4][8].

The diagnosis of flat feet in children generally uses traditional methods such as wet footprint tests, X-rays, or MRIs. However, these methods often require high costs, expensive equipment, and radiation exposure that can be risky for children, especially in the use of X-rays and MRIs, which require a lot of time and money for diagnosis [9][8]. On the other hand, manual footprint analysis using the Foot Posture Index (FPI-6) can be influenced by subjectivity, leading to variations in diagnostic results, especially in uncooperative children or those with uncertain posture [10][1].

Clarke's Angle is one of the methods that has been proven to be highly effective in identifying the degree of flat feet in children. Based on a study conducted by Hegazy et al. (2021), Clarke's Angle demonstrates very high diagnostic accuracy, with a sensitivity of 98% and specificity of 99%, making it one of the most reliable methods for assessing flat feet in children. An Area Under the Curve (AUC) of 0.98 indicates a very high predictive ability in distinguishing flat feet from normal feet, which is crucial for avoiding misdiagnosis[11]. Clarke's Angle measurement is performed by measuring the angle formed between the lines connecting specific points on the foot. A decrease in this angle indicates a deformity of the foot known as flat feet. This method offers significant advantages over other methods, such as the Foot Posture Index (FPI-6), which has an AUC of 0.80, lower than Clarke's Angle, which provides a higher and more consistent AUC in diagnosis.

Based on the latest developments, significant research gaps have been identified in the practicality and accessibility of diagnostic systems. The study by Kalghatgi et al. (2025) has proven the reliability of morphological indices for detecting pes planus, demonstrating excellent accuracy with established indices like Clarke's Angle, Chippaux-Smirak Index, and Staheli Index. However, the study faced significant operational constraints, particularly in terms of scanning time, which took approximately one minute per patient. This extended duration poses a serious obstacle when dealing with pediatric patients who have difficulty remaining still for prolonged periods due to their limited attention span and inability to maintain stable posture[4]. Moreover, the system requires additional post-processing time after image capture for stitching, segmentation, and index calculation before results become available, further extending the total examination time and increasing the likelihood of patient discomfort or movement during the waiting period.

Addressing these critical limitations, we developed an integrated web-based system that not only maintains the accuracy of Clarke's Angle measurements but also incorporates IoT technology for real-time weight measurement and, most importantly, delivers instantaneous diagnostic results. Unlike existing systems that require post-processing workflows where patients must wait for image analysis to complete, our platform performs real-time Clarke's Angle calculation displaying results immediately upon footprint image capture and

Jurnal Teknik Informatika Vol. 19 No. 1, April 2026 (1-11)
ISSN: p-ISSN 1979-9160 (Print)| e-ISSN 2549-7901 (Online)
DOI: https://doi.org/10.15408/jti.v19i1.47091

storage. This means that the moment a child's footprint image is successfully captured and measurement data is saved, the Clarke's Angle value is instantly visible to the clinician, eliminating any waiting time between examination and diagnosis. This real-time processing capability is particularly crucial for pediatric populations, where minimizing total examination time is essential for obtaining reliable measurements from young, often uncooperative patients who may become restless during prolonged procedures. The web-based architecture enables rapid, accurate, and non-invasive diagnosis, reducing reliance on expensive imaging equipment and invasive procedures commonly used in traditional diagnostic methods [12][13].

This system represents a significant leap forward by integrating technology that enables instantaneous diagnosis while eliminating errors caused by subjectivity often found in manual methods. The automated, real-time Clarke's Angle analysis produces immediate, accurate, and consistent results, making it beneficial not only for individual pediatric consultations but also for mass screening programs and school health assessments where rapid turnaround time and efficient workflow are essential for early detection and timely intervention.

2. METHODS

2.1. Design Hardware

This device is called the F-scale and is designed using iron plates as its basic structure to provide optimal strength and stability, capable of withstanding loads of more than 200 kg, ensuring excellent stability during shooting. The use of iron plates also aims to provide parents with a sense of security, so they can feel confident that their children will be safe when using the F-scale. With its sturdy structure, this device can support the weight of a child without the risk of instability or damage. In addition, we also invite parents to try this device so they can experience its safety and reliability firsthand. A webcam Akona with a 4K lens and 1080P HD resolution is mounted at a height of 30 cm from the surface of the base. This height was chosen based on calculations of the camera's 150-degree viewing angle, which allows the entire foot area to be captured clearly and in detail. At a height of 30 cm, the camera can capture images optimally without sacrificing sharpness, while maintaining focus on the foot area, which is the object of analysis. This webcam is equipped with a Flagship 6.0 image processor and auto-focus feature to produce precise images. In addition, this camera is capable of reaching a frame rate of 30FPS, with 360° horizontal rotation and ±15° vertical tilt capabilities, providing flexibility in capturing images from various angles. The device's connectivity uses a plug-and-play system without requiring additional drivers, and a USB interface with a 1.5-meter cable length. Green LED lighting is used, as seen in Figure 1, to provide even lighting across the entire foot area.

Figure 1. *F-scale with Camera and LED Lighting*

2.2. Design System

This study aims to design and implement a web-based system that can automatically detect the type of foot arch in children using Clarke's Angle. This system integrates body weight measurements using the F-Scale with foot images captured via webcam or uploaded files, then analyzes these images to calculate Clarke's Angle as an indicator of foot type (flat, normal, or high).

This system is built with a web-based user interface that allows users to select the image capture method (from uploaded files or via webcam in real-time), as well as utilize the HTTP PUT API for communication between the scale and the web application. Figure 2 shows the system architecture diagram that illustrates the workflow between the scale, camera, and website in the process of examining and classifying foot arch types.

The architecture of this Child Health Examination Management System integrates a front-end website, back-end server, IoT devices, and a database to streamline the child

Jurnal Teknik Informatika Vol. 19 No. 1, April 2026 (1-11)
ISSN: p-ISSN 1979-9160 (Print)| e-ISSN 2549-7901 (Online)
DOI: https://doi.org/10.15408/jti.v19i1.47091

health examination process. Healthcare professionals use the website to manage data, fill out forms, and view examination history, while IoT devices such as the F-Scale, LILA Measurement Tool (for measuring arm circumference, head circumference, and height), and USB camera send data to the server via an API. The back-end, built with Laravel, processes this data, including image analysis, and stores it in a MySQL database. Laravel, a well-known PHP framework, simplifies web application development, making it easy to access through a browser without installation [14]. MySQL ensures that data can be easily accessed and securely managed, allowing the system to handle large amounts of data efficiently.

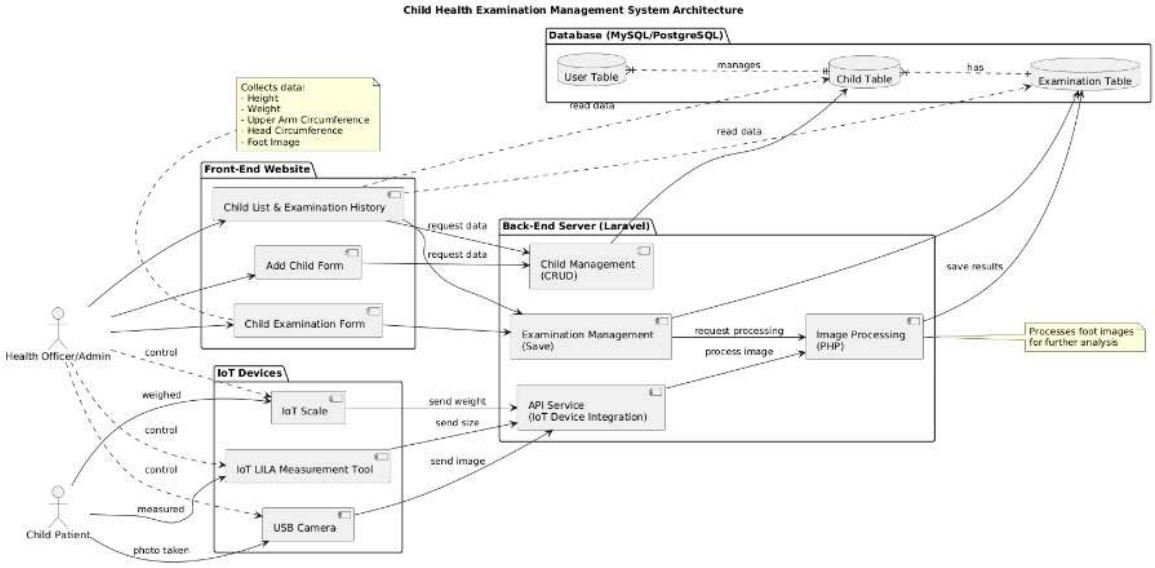

Figure 2. *System Architecture Diagram*

2.3. Image Processing

The automated image processing system uses a detailed multi-stage algorithm to precisely measure Clarke's Angle from plantar footprint images. Figure 3 illustrates the key steps in the workflow, starting from image capture and ending with the final measurement. The process kicks off with input validation, checking images from a webcam or uploaded files for JPEG or PNG compatibility. It reads metadata to confirm file integrity and gather size details before moving forward. A key addition here is automatic background removal, which separates the foot's anatomical features from irrelevant surroundings, boosting efficiency and precision [15]. Footprint images often include distractions like platform edges or floor details that could skew results. Medical images frequently have unnecessary parts, so preprocessing is essential to clean them up, aiding segmentation and feature extraction. The system applies a smart background segmentation method that spots and isolates the footprint while filtering out noise. It uses adaptive thresholding with connected component analysis to separate the foot from artifacts, dividing the image into foreground and background based on a threshold. Removing background early ensures better feature detection and more accurate landmark spotting for Clarke's Angle later. This is especially useful in clinics with varying conditions, keeping measurements consistent.

Next, the system uses the Features from Accelerated Segment Test (FAST) algorithm for corner detection and keypoint finding [16]. It examines pixel intensity to spot important features across the footprint, laying the groundwork for edge detection and structural review. Adjustable thresholds help pinpoint points that define foot shapes and key anatomical spots, improving accuracy in later steps. After that, images convert to grayscale with standard filters. This simplifies analysis by cutting out color interference. The result is a

ISSN: p-ISSN 1979-9160 (Print)| e-ISSN 2549-7901 (Online)
DOI: https://doi.org/10.15408/jti.v19i1.47091

single-channel image with intensity from black (zero) to white (maximum), speeding up computations while keeping vital structural details. On the grayscale image, the system performs tone analysis, building an intensity map by checking each pixel's value. It averages intensity across the image and creates a map showing pressure areas: high pressure as solid contact (dark), moderate as arch regions (medium), and no contact as background (light). This is crucial for arch detection, where the medial longitudinal arch shows intermediate values. Then, it applies Otsu's automatic thresholding, which analyzes the histogram to maximize variance between classes and find the best threshold [17][18]. It sets a main threshold for foot vs. background, then secondary ones at 70% and 130% for arch areas. This multi-level approach defines object edges and distinguishes regions by intensity, enabling precise segmentation for Clarke's Angle. With these thresholds, the image gets segmented into three levels: solid foot contact (black), arch areas (gray), and background (white). Segmentation outlines key parts, splitting the image into foreground and background based on thresholds[19]. It produces two images: a binary one for foot vs. background, and one for arch zones. The arch map highlights partial contact areas, vital for landmark detection. To clean up, morphological operations use erosion and dilation to handle connectivity—erosion shrinks by removing boundary pixels, dilation expands by adding them. For arches, it keeps regions with at least three connected neighbors (arch or foot), removing noise while preserving structure. Connected component analysis with dilation identifies continuous areas, eliminating loose bits. For solid regions, erosion keeps only fully connected pixels. These steps reduce noise, sharpen edges, and yield accurate contours. The image then rotates 90 degrees counterclockwise to align the foot with toes up and heel down, standardizing for landmark detection. This avoids angle variations and ensures consistency. The system finds the smallest rectangle around the foot by locating extreme pixels in solid and arch areas, giving foot length (horizontal) and width (vertical). These help confirm detection and provide baselines for analysis. Inside this box, arch detection scans horizontal lines in the middle 50% of the foot (25% to 75% height). For each line, it calculates the arch-to-solid pixel ratio and an arch score based on width and ratio. The lowest score marks the arch landmark, with medial and lateral points identified there—the medial one key for Clarke's Angle. This works even for subtle arches. Heel detection checks the bottom 10 pixels, finding the lowest line with contact, then the midpoint between left and right edges. This handles irregular heels reliably. Toe detection adapts based on arch side: left-to-right search if medial, right-to-left if lateral, within the top 10 pixels, to find the medial toe boundary. With toe, arch, and heel points set, Clarke's Angle is calculated geometrically. Vectors from arch to toe and arch to heel give the angle via dot product and magnitudes, converted to degrees. It's 180 degrees minus this angle, matching clinical definitions. Angles under 30 degrees mean flat foot (pes planus), 30-45 degrees moderate arch, over 45 degrees high arch (pes cavus). The system checks for 0-180 degree range, flagging anomalies. Finally, it creates visual outputs: an annotated image with colored landmarks and angle lines. These save with timestamps alongside numbers for records and review. The entire pipeline operates in real-time, making it perfect for pediatric use by reducing both manual variability and time compared to traditional methods.

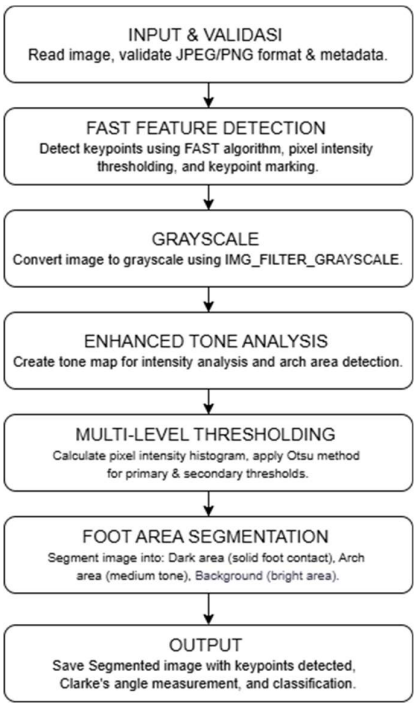

Figure 3. *Block diagram of image processing steps*

Jurnal Teknik Informatika Vol. 19 No. 1, April 2026 (1-11)
ISSN: p-ISSN 1979-9160 (Print)| e-ISSN 2549-7901 (Online)
DOI: https://doi.org/10.15408/jti.v19i1.47091

2.4. Calculation of Clarke's Angle

After the foot image has been successfully processed and the sole area identified, Clarke's Angle is calculated based on the coordinates of three points located on the relevant part of the sole:

a. Point S (Start): The most medial point of the heel of the foot.
b. Point T (Toe): The most lateral point of the toe
c. Point F (Foot): The point in the middle of the sole of the foot, usually connected to the metatarsal and medial parts.

Clarke's Angle is calculated by measuring the angle between two lines:

a. First line: The line connecting point S (medial heel) and T (lateral toe).
b. Second line: The line connecting T (lateral toe) and F (medial metatarsal).

The positions of points S, T, and F are illustrated in the figure 4, with the lines formed between these points used to calculate the angle.

The mathematical formula for calculating the angle between the two lines formed by these points is:

$$CA = 180° - cos^{-1}\left(\frac{(x_T - x_S)(x_F - x_S) + (y_T - y_S)(y_F - y_S)}{\sqrt{(x_T - x_S)^2 + (y_T - y_S)^2} \cdot \sqrt{(x_F - x_S)^2 + (y_F - y_S)^2}}\right) \quad (1)$$

Where:

- (x_T, y_T) are the coordinates of point T (toe)
- (x_F, y_F) are the coordinates of point F (foot)
- (x_S, y_S) are the coordinates of point S (heel)

Clarke's Angle is calculated using the inverse cosine function ($\cos^{-1}$) to find the angle between the two lines connecting these points. This angle value is used to classify the type of foot curvature [20]:

- If Clarke's Angle is less than 30°, the foot is categorized as flat foot (pes planus).
- If Clarke's Angle is between 30° and 45°, then the foot is categorized as normal.
- If Clarke's Angle is greater than 45°, then the foot is categorized as high arched (pes cavus).

Figure 4. *The lines formed between points S, T, and F are used to calculate Clarke's Angle*

3. RESULTS AND DISCUSSION

This website was tested at two locations in Semarang City, namely the Habibie Ainun Tlogosari Kindergarten & Daycare and the Kemuning Integrated Health Service Post. A total of 180 children participated in the study, with 150 children from the Habibie Ainun facility and 30 children from the Kemuning Integrated Health Service Post. The subjects' ages ranged from 2 to 7 years, representing the critical period of medial longitudinal arch (MLA) development in childhood. This age range was chosen based on the physiological characteristics of children's foot development, as the arch of the foot begins to form significantly during this period.

3.1. Prevalence of Foot Conditions in Children

The test results from both research locations showed varying distributions of foot arch types among the 180 research subjects. Table 1 presents a comprehensive distribution of foot conditions identified through a web-based system using Clarke's Angle method.

Table 1. *Distribution of Foot Arch Types in Research Subjects*

Classification of Foot Conditions	Number of Subjects (n)	Percentage (%)
Flatfeet (Pes Planus)	58	32,22
Normal	120	66,67
Pes Cavus (High Arch)	2	1,11

The data in Table 1 shows that the majority of research subjects (66,67%) showed foot arch development that was in the normal

Jurnal Teknik Informatika Vol. 19 No. 1, April 2026 (1-11)
ISSN: p-ISSN 1979-9160 (Print)| e-ISSN 2549-7901 (Online)
DOI: https://doi.org/10.15408/jti.v19i1.47091

category. However, a significant proportion, namely 27.78% of subjects, were identified as having flat feet. This finding indicates the importance of implementing early detection in this age group to prevent potential biomechanical disorders and postural abnormalities that can continue into adulthood. The prevalence of pes cavus showed a minimum value of 1.11%, which is consistent with the literature that this condition is relatively rare in the pediatric population.

3.2. Distribution Analysis Based on Research Location

The distribution of test results at both research locations is presented in Table 2. Analysis based on location aims to identify potential demographic variations or environmental factors that may influence the pattern of foot arch development in research subjects.

Table 2. *Distribution of Foot Conditions Based on Research Location*

Research Location	Flatfeet (n)	Normal (n)	High Arch (n)	Total (n)	Prevalence of Flat Feet (%)
Kindergarten & Daycare Tlogosari	50	100	0	150	33.33
Integrated Service Post Kemuning	8	20	2	30	26.67

The prevalence of flat feet was slightly higher in kindergartens and childcare centers (33.33%) compared to integrated health posts (Posyandu) (26.67%). This variation may reflect demographic differences or environmental factors influencing foot development. It is noteworthy that all cases of high arched feet were identified at Posyandu, although the small sample size requires careful interpretation. The relatively high prevalence of flat feet in both locations underscores the need for ongoing monitoring and early intervention strategies to support proper musculoskeletal development during these formative years.

3.3. System Validation Using the Wet Footprint Test Method

The accuracy of the web-based system was validated through comparative measurements using the wet footprint test, a conventional method for diagnosing flat feet. All research subjects (n=180) underwent both measurement methods sequentially to ensure the validity and reliability of the developed system. Figure 5(a) shows the original image captured from the webcam after passing through input and validation processes, including background removal. Figure 5(b) shows the result from the web-based system, where Clarke's Angle is automatically calculated from the foot's shape. In contrast, Figure 5(c) shows the result from the traditional wet footprint test, which requires subjects to step on an ink-moistened pad to create a footprint, from which Clarke's Angle is measured manually.

(a)

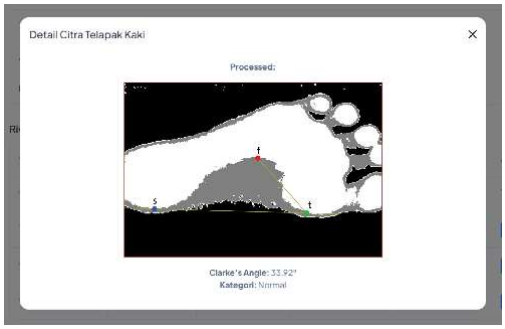

(b)

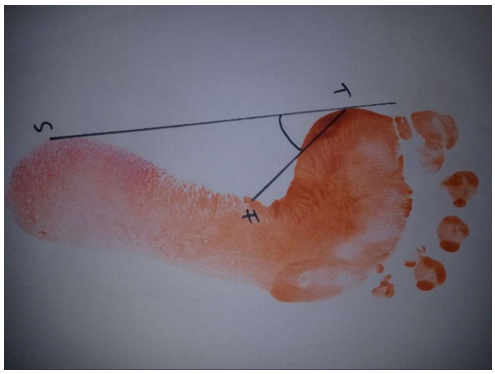

(c)

Figure 5. *Comparison between the web-based system and the traditional wet footprint test for measuring Clarke's Angle. (a) shows the original image captured from the webcam, (b) shows the result from the web-based system, and (c) shows the result from the traditional wet footprint test*

In addition, the comparison between these two methods also aims to assess the

ISSN: p-ISSN 1979-9160 (Print)| e-ISSN 2549-7901 (Online)
DOI: https://doi.org/10.15408/jti.v19i1.47091

efficiency and practicality of web-based systems in clinical applications. The wet footprint method requires a more time-consuming manual process and can be influenced by external factors, such as ink quality or the accuracy of the subject when stepping. In contrast, web-based systems offer a faster, automated process that is independent of external factors, enabling more consistent and repeatable measurements. Although both methods show a high level of agreement in measuring Clarke's Angle, web-based systems offer advantages in terms of practicality and precision, which are particularly important in diagnosing flat feet in a wider population.

3.4. Comparative Analysis of Measurement Results

A comparative analysis between the web-based system and the wet footprint test method showed a high level of concordance in Clarke's Angle measurements across all 180 research subjects. Table 3 presents representative data from Clarke's Angle measurements obtained from both methodologies on a randomly selected sample of subjects. Figure 6 presents the comparison between the results from the web-based system and the wet footprint test. The graph shows how both methods yielded similar outcomes across the sample, further emphasizing the minimal deviation between the two measurement techniques.

Table 3. *Representative Sample Comparison of Clarke's Angle Measurements: Web-Based System vs. Wet Footprint Test*

Code	Age (month)	Website Results	Wet Footprint test results	Absolute Difference (°)	Percentage Deviation (%)
TKA1	58	38,45	38,90	0,45	1,17
TKB1	69	36,75	37,15	0,40	1,09
PSYD1	95	54,39	46,50	0,30	0,65
DYCR1	31	28,90	29,15	0,25	0,86
DYCR2	35	27,45	27,80	0,35	1,27
PSYD2	68	44,30	44,05	0,25	0,56
PSYD3	68	33,92	33,10	0,32	0,78
TKA2	50	39,80	40,15	0,35	0,88
TKB2	68	31,75	32,10	0,35	1,10
TKB3	69	42,10	41,85	0,25	0,60
TKA3	53	35,60	35,95	0,35	0,98

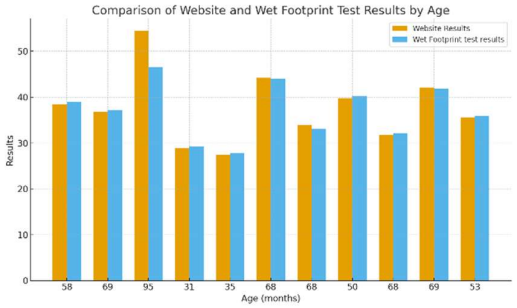

Figure 6. *Comparison between the results from the web-based system and the wet footprint test*

The analysis results show that the measurement deviation between the two methods is minimal across all 180 subjects, with an average absolute difference of 0.34° ± 0.12° and an average percentage deviation of 0.93% ± 0.35%. As an illustration, in Sample S001, where the web-based system measured Clarke's Angle at 40.88°, the wet footprint test method produced a value of 41.20°, with a difference of only 0.32° or equivalent to a deviation of 0.78%. This level of precision is within the acceptable range of clinical measurement error and indicates the high reliability of the developed system.

3.5. Consistency of Diagnostic Classification

The consistency evaluation of the classification shows that the web-based system is capable of producing diagnoses that are congruent with the wet footprint test method in all 180 subjects. Although there was minimal numerical variation in Clarke's Angle measurements, this difference did not result in discrepancies in foot condition classification because the variation remained within the threshold range set for each category (flat feet: <30°, normal: 30-45°, pes cavus: >45°). Sensitivity and specificity analysis of the system showed that the web-based system successfully classified foot arch conditions with 98.89% accuracy when compared to the gold standard wet footprint test.

Of the 180 subjects tested, there were only 2 misclassification cases: 1 subject classified as pes planus by the web-based system but identified as normal by the wet footprint test (Clarke's Angle: 29.85° vs. 30.15°), and 1 subject classified as normal by the web-based system but identified as pes planus by the wet footprint test (Clarke's Angle: 30.25° vs. 29.90°). Both cases were in

ISSN: p-ISSN 1979-9160 (Print)| e-ISSN 2549-7901 (Online)
DOI: https://doi.org/10.15408/jti.v19i1.47091

the borderline classification threshold zone (around 30°), which explains the minimal difference in interpretation between the two methods.

This system provides real-time results, making it easier for medical personnel to immediately provide information related to children's foot conditions. Although there are some limitations, such as dependence on image quality, the test results show that this system can be used effectively in a wider environment, especially in schools or health centers to detect foot problems in children early on.

While the web-based system shows promising results in detecting Clarke's Angle and classifying foot types in children, there are several limitations that need to be considered. One of the main limitations is the quality of the images taken. Clarke's Angle measurements are highly dependent on the quality of the images obtained from the webcam. Inadequate lighting, improper foot positioning, and image distortion due to subject movement during image capture can cause errors in segmentation and detection of points on the sole of the foot. This can certainly affect the results of foot type measurement and classification, especially in cases of feet with very low or high arches, which require very precise measurements. Additionally, the accuracy of the system also heavily depends on the position of the feet during image capture. This system assumes that the subject is standing in the correct position, with their feet flat on the weighing device. Any misalignment or shift of the feet from the ideal position can result in errors in angle measurement and lead to incorrect classification.

A remaining limitation of the current system is its reliance on single-view 2D plantar images, which may not capture subtle variations in arch contour that are better represented in surface-rich data. To enhance measurement robustness and reduce sensitivity to lighting conditions and foot placement, future work will explore the integration of depth-sensing (RGB-D) cameras. Such devices can record the plantar region together with depth information, allowing derivation of parameters such as navicular height and plantar surface depression, thereby providing a closer approximation of the actual foot morphology. In addition, subsequent versions of the system should incorporate automated validation of foot position and weight-bearing using pose-estimation techniques, so that images are acquired only when the subject stands in an appropriate posture. This is expected to minimize user-induced variability and improve the consistency of arch-type classification, particularly in pediatric screening settings.

CONCLUSION

This study successfully addresses key challenges in diagnosing pediatric flatfoot by developing a practical and accessible web-based system. By integrating Clarke's Angle measurement with real-time data processing, the system offers a more efficient and cost-effective solution compared to traditional methods like radiography or manual footprint analysis, which often require expensive equipment and can yield inconsistent results due to operator subjectivity. The system's core strength lies in its ability to accurately classify foot arch types (normal, flat, or high) with remarkable speed. This is achieved through a synergistic combination of the robust F-Scale hardware and a sophisticated image-processing algorithm that performs objective, automated Clarke's Angle calculations. Crucially, the platform delivers diagnostic results the instant a footprint image is captured, a vital advancement for managing young, often uncooperative patients who cannot remain still for long periods. Validation tests confirm the system's high reliability, demonstrating an excellent match with the conventional wet footprint test and a classification accuracy of 98.89%. This performance establishes the system as a viable and advanced tool for both clinical and community-based settings. The immediate application of this technology holds the potential to revolutionize early screening programs. Its implementation in schools and integrated health posts would enable rapid, non-invasive mass screenings to identify children at risk of persistent pes planus. This facilitates timely intervention, which is key to preventing long-term musculoskeletal complications. To further advance this work, future research will focus on integrating depth-sensing (RGB-D) cameras to capture three-dimensional foot morphology, such as navicular height, which would provide a more comprehensive

biomechanical assessment. Additionally, we are developing real-time posture validation algorithms using pose estimation to automatically correct for foot misplacement, enhancing measurement accuracy and consistency. The ongoing development of this system signifies a pivotal step towards intelligent, accessible pediatric musculoskeletal screening.

REFERENCES

[1] H. Jiang *et al.*, "Understanding foot conditions , morphologies and functions in children : a current review," no. July, pp. 1–11, 2023, doi: 10.3389/fbioe.2023.1192524.

[2] C. Bagley *et al.*, "FULL PAPER MRI for paediatric flatfoot : is it necessary ?," no. November 2021, pp. 1–7, 2022.

[3] M. Ghorbani and R. Yaali, "The impact of flatfeet on the correlation between functional movement scores , balance , agility , and core muscle strength in young females : a cross-sectional study," pp. 1–8, 2025.

[4] K. Kalghatgi and K. Verma, "Flatfoot Detection in an Indian Population : Validation of Morphological Indices Using a Diagnostic Device †," pp. 1–7, 2025.

[5] G. Giuca, D. A. Marletta, B. Zampogna, I. Sanzarello, M. Nanni, and D. Leonetti, "Correlation Between the Severity of Flatfoot and Risk Factors in Children and Adolescents : A Systematic Review," pp. 1–16, 2025.

[6] Y. Hoseini and M. Taghi, "Journal of Bodywork & Movement Therapies Ground reaction force analysis in flexible and rigid flatfoot subjects," *J. Bodyw. Mov. Ther.*, vol. 39, no. January 2023, pp. 441–446, 2024, doi: 10.1016/j.jbmt.2024.02.020.

[7] Y. Umardani, D. B. Wibowo, W. Caesarendra, and A. Suprihanto, "applied sciences Calculation of the Rearfoot Angle Representing Flatfoot from Comparison to the Cavanagh Arch Index," 2022.

[8] M. Bouchard and T. D. Ross, "Bony Procedures for Correction of the Flexible Pediatric Flatfoot Deformity," 2021, *Elsevier Inc*. doi: 10.1016/j.fcl.2021.09.001.

[9] R. Berkeley, S. Tennant, A. Saifuddin, and R. Berkeley, "Multimodality imaging of the paediatric flatfoot both underlying causes and potential surgically correctable," *Skeletal Radiol.*, pp. 2133–2149, 2021, doi: 10.1007/s00256-021-03806-8.

[10] F. A. Hegazy, E. A. Aboelnasr, Y. Salem, and A. A. Zaghloul, "Musculoskeletal Science and Practice Validity and diagnostic accuracy of foot posture Index-6 using radiographic findings as the gold standard to determine paediatric flexible flatfoot between ages of 6 – 18 years : A cross-sectional study," *Musculoskelet. Sci. Pract.*, vol. 46, no. January 2020, p. 102107, 2020, doi: 10.1016/j.msksp.2020.102107.

[11] F. Hegazy, I. Kim, and Y. Salem, "Comparing Validity and Diagnostic Accuracy of Clarke ' s Angle and Foot Posture Index-6 to Determine Flexible Flatfoot in Adolescents : A Cross-Sectional Investigation," no. July, 2021.

[12] Z. Yu *et al.*, "Exploring flatfeet morphology in children aged 6 – 12 years : relationships with body mass and body height through footprints and three - dimensional measurements," *Eur. J. Pediatr.*, pp. 1901–1910, 2024, doi: 10.1007/s00431-024-05471-0.

[13] C. Drake *et al.*, "Medical imaging for plantar heel pain : a systematic review and meta-analysis," vol. 2, pp. 1–18, 2022.

[14] B. Kurniawan, "Aplikasi Pemesanan Makanan Di Bebek dan Ayam Tekaeng Menggunakan Php dan Mysql".

[15] C. Dindorf *et al.*, "Toward automated plantar pressure analysis : machine learning-based segmentation and key point detection across multicenter data," no. June, pp. 1–16, 2025, doi: 10.3389/fbioe.2025.1579072.

[16] S. Budzan and R. Wy, "Performance Analysis of Keypoints Detection and Description Algorithms for Stereo Vision Based Odometry," 2025.

[17] J. R. Informatika, "IMAGE SEGMENTATION ANALYSIS USING OTSU THRESHOLDING AND," vol. 6, no. 1, 2023.

[18] V. Thamilarasi, A. Asaithambi, and R. Roselin, "ENHANCED ENSEMBLE SEGMENTATION OF LUNG CHEST X-RAY IMAGES BY DENOISING AUTOENCODER AND CLAHE," vol. 9102, no. February, pp. 3501–3508, 2025, doi: 10.21917/ijivp.2025.0496.

[19] J. Li and X. Gui, "applied sciences Fully Automatic Grayscale Image Segmentation : Dynamic Thresholding for Background Adaptation , Improved Image Center Point Selection , and Noise-Resilient Start / End Point Determination," 2024.

[20] Y. Latifah, A. F. Naufal, D. Nafi, and R. W. Astari, "Hubungan Antara Postur Flat Foot Dengan Keseimbangan Statis Pada Anak Usia 12 Tahun," vol. 2, no. 1, pp. 1–6, 2021.